Performance evaluation of titanium oxide deposited by electrophoresis in photoelectrodes of dye-sensitized solar cells

Antonio Paulo Santos Souza [1], Natália Macêdo Cavalcante [2],
Francisco Nivaldo Aguiar Freire [2], Ana Fabíola Leite Almeida [2]

[1] Department of Engineering and Materials Science, Ceara Federal University - UFC, Avenue Humberto Monte-Pici, Block 729, CEP: 60455-900, Fortaleza, Ceara, Brazil.
[2] LAFFER - Thin Films Laboratory in Renewable Energy, Mechanics Engineering Department, Ceara Federal University - UFC, Avenue Humberto Monte-Pici, Block 715, CEP: 60455-900, Fortaleza, Ceara, Brazil.
e-mail: antonio.souza@fisica.ufc.br, nataliacav@gmail.com, nivaldo@ufc.br, anfaleal@yahoo.com.br

ABSTRACT

Nanoparticles of TiO_2 have been the main semiconductor applied in Dye-sensitized solar cells (DSSCs). In this work, solar cells were developed from the electrophoretic deposition of anatase titanium dioxide (TiO_2) films on conductive glasses. The electrophoretic deposition was perfomed with a constant voltage of 80V for 2 minutes and, after drying, the films were sintered at three different temperatures: 450 °C, 550 °C and 600 °C. In the assembly of the cells, the titanium dioxide films were sensitized by Ruthenizer 535-bisTBA dye (N719) and an electrolyte containing the iodide / tri-iodide redox pair and a commercial transparent platinum counter electrode were used. TiO_2 films were characterized by scanning electron microscopy, dispersive energy spectroscopy and X-ray diffraction and photo-electrochemical techniques. The energy conversion rates were 0.2646% for the sintered film at 450 °C, 0.1209% for the sintered film at 550 °C and 0.1137% for the film sintered at 600 °C.

Keywords: Dye-sensitized solar cells. Electrophoresis. Titanium dioxide. Film. Mesoporous. Photoanode.

1. INTRODUCTION

The crystalline titanium dioxide (TiO_2), which is a semiconductor with energy *gap* in the ultraviolet region [1-3], owns excellent optical and electrical properties and to this day is vastly studied for numerous applications such as pigment [4], photocatalysis [5], gas sensor [6], sunscreen [7] and dye-sensitized solar cell (DSSC) [8] due to its unique optoelectronic features. Dye-sensitized solar cells are considered one of the most promising of the new generation of cells, due to the low cost of manufacture compared to silicon cells, and their development is in continuous progress [9]. These cells are conventionally build with a nanoporous layer of a semiconductor material of large *gap*, usually TiO_2 [7], ZnO [10, 11] or SnO_2 [12], covered by a layer of photoexcited dye, generally the dyes with Ruthenium (II) poly pyridine complex. [13, 14] The work electrode is connected to a counter electrode of catalytic material (Platinum, gold or activated coal) through an electrolyte with a iodide/triiodide redox pair (usually $3I^-/I_3^-$) which holds good stability and reversibility. [15, 16] Highly porous layers of titanium dioxide can be produced by a number of techniques such as doctor blade [10], electrospinning [17], sputtering [18], micro-plasma oxidation [19] and electrophoretic deposition [8]. Because of the combinations of the high versatility of its use with different materials and cost-effectiveness, the electrophoretic deposition (EPD) technique, with a wide range of novel applications in the processing of advanced ceramic materials and coatings, has recently gained increasing interest in academia and industrial sector. [20, 21] In EPD, charged powder particles, dispersed or suspended in a liquid medium are attracted and deposited onto a conductive substrate of opposite charge under the application of a DC electric field.[22, 21] In EPD, charged powder particles, dispersed or suspended in a liquid medium are attracted and deposited onto a conductive substrate of opposite charge under application of a DC electric field. [22, 21]

Given the above, the present work aims to evaluate the performance of solar cells sensitized by the dye N719, which use a TiO_2 film, deposited by the electrophoresis technique and treated with different sintering temperatures, as the photoanode. Measurement of the crystalline structure of the films by X-ray diffraction simultaneously with the calcination process. In addition: to characterize the semiconductor oxide films by

means of Scanning Electron Microscopy (SEM); Dispersive Energy Spectroscopy (EDS) and current-voltage (J-V) density plots.

2. MATERIALS AND METHODS

All chemicals (reagent grade: Sigma-Aldrich, Dynamics and Vetec) were used as received, without further purification processes. All solutions were prepared with deionized water.

2.1 Preparation of the electrodes with TiO$_2$

The method for the preparation of the electrodes with commercial TiO$_2$ nanoparticles is known [8, 23-25]. Initially, a larger area of the FTO surface received the TiO$_2$ nanoparticles by the electrophoretic process. Following, from this area, it was limited an effective area, which, would be, afterwards, used on the fabrication of the studied devices.

2.2 Equipment and experimental techniques

2.2.1 Scanning Electron Microscopy (SEM) and Energy-dispersive x-ray spectroscopy (EDS)

The SEM and EDS measures were done by the scanning electron microscope (Inspect S50 – FEI) with an EDS detector connected. The measurement conditions were: working distance (WD) of 11.7 mm and accelerating voltage of 20 kV.

2.2.3 X-Ray Diffraction (XRD)

X-ray diffraction measures for phase identification were performed on a Bruker D8 Advance device, with CoKα1 (λ = 0.1789 nm) as the radiation source and using a voltage of 40kV, a current of 40mA and an angular variation of 20°-75°. A thermal chamber was attached to this equipment so that the measurements could be monitored simultaneously with the gradual increase in temperature.

2.2.4 Photoelectrochemical characterization of the solar cells.

For all the assembled DSSCs, electric measurements were made by two electrodes potentiostat using 100 mW/cm^2 light source of Led white-neutral. The electrical parameters and current-voltage (J_{SC} - V_{OC}) density curves, in addition to the parasitic resistances, were obtained based on the circuit model proposed by VITALL *et al.* [26] in order to obtain the efficiencies of the cells. All data of the curves (J-V) are shown in Table 5.

All the measurements were performed to environment temperature on a dye-sensitized solar cell, using the N719 dye, supplied by Solaronix. The light source was a triple LED array driven by the output current of 400mA of the Autolab LED Driver. The output of the LED Driver is controlled by the DAC164 of the Autolab, directly from the software. All the measurements were carried out with the NOVA software. The cells were fixed to distance 13 cm of the light source.

2.2.5 Electrophoretic Deposition

All the films holding the nanostructures were deposited in a conductive glass (FTO- SOLEMS®) [27] with resistance varying between 50.0 –70.0 Ω/cm^2. The substrates were previously cleaned using the following solvents: deionized water, acetone and isopropyl alcohol, in this sequence. The conductive substrates were kept immersed for 15 minutes on ultrasonic bath, for each solvent.

For the deposition of the TiO$_2$ film on the glass substrate with FTO, an electrophoresis source with a maximum voltage of 300 V and a maximum current of 700 mA of the Kasvi brand was used. A suspension was prepared containing 0.04 g of TiO$_2$ anatase from the Sigma-Aldrich® brand dispersed in a solution containing 10 ml of acetone and 30 ml of isopropyl alcohol. Then, a solution was prepared with 0.18 g of resublimated iodine and 50 ml of acetone. The suspension and solution were mixed and subjected to magnetic stirring and ultrasonic vibration for 20 minutes.

Equation 1 shows that the reaction of iodine with acetone has hydrogen ions as one of the products and, according to SOUZA *et al.* (2018) [15], the presence of H$^+$ ions increases the conductivity of the suspension.

$$CH_3-CO-CH_3{}_{(aq)} + 2I_2{}_{(aq)} \leftrightarrow ICH_2-CO-CH_2I + 2H^+{}_{(aq)} + 2I^-{}_{(aq)} \tag{1}$$
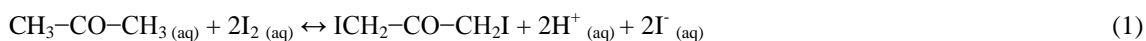
The positive electrode used the conductive glass with FTO mentioned above and the counter electrode used a commercial platinum substrate with a distance of 3 cm between them. Electrophoretic deposition was carried out with a constant voltage of 80V for 2 minutes. Figure 1 shows the process illustration for the electrophoresis deposition. At the end of the deposition, drying was carried out at 100 °C. After this procedure, the TiO_2 films were sintered at three different temperatures: 450 °C, 550 °C and 600 °C, with a heating rise of 30 °C/ min. Therefore, the samples remained at the respective temperatures for a period of 30 minutes.

Several studies have shown that the sintering temperature for an optimal degree of crystallinity of the TiO2 film deposited on FTO is around 450 ° C. This optimal pattern of crystallinity is associated with greater efficiency of dye-sensitized solar cells. [28-31]

The samples containing a TiO_2 anatase film sintered at different temperatures were called sample 450, sample 550 and sample 650 for the sintering temperatures of 450 °C, 550 °C and 600 °C respectively (Table 1).

Table 1: Samples of TiO_2 anatase films sintered at different temperatures.

SAMPLE 450	SAMPLE 550	SAMPLE 600
Sintered at 450 °C	Sintered at 550 °C	Sintered at 600 °C
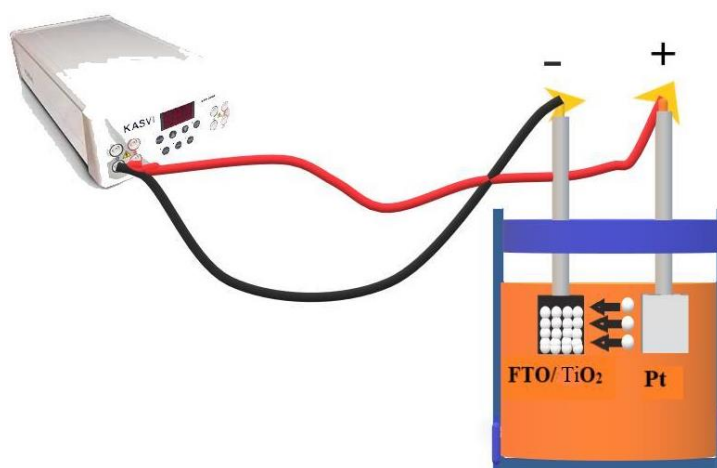
Figure 1: Illustration of the electrophoretic deposition.

Lastly, the deposited films by electrophoresis were used as photoanodes of dye-sensitized solar cells as detailed as follows.

2.2.6 Assemble of the dye sensitized solar cells

After thermal treatment, the samples with the TiO_2 nanostructures also were under ethanol solution ($3x10^{-4}$ mol L^{-1}) of the "Ruthenizer 535-bisTBA" (N719) [32] dye for 24 hours. After, the films were washed in ethanol to extract the dye concentrated in the surface, due to an incomplete adsorption. After drying at room temperature, the electrodes were placed in touch through a commercial [32] redox pair electrolyte (iodide/triiodide) with an counter electrode [32] also commercial containing a thin platinum layer deposited on FTO. The commercial selant [32] was used to avoid the leaking of the electrolyte from the cell.

3 RESULTS AND DISCUSSION

3.1 Morphological analysis with MEV/EDS

TiO_2 films were analyzed morphologically using the scanning electron microscopy technique.

Figure 2 shows the surface morphology of TiO_2 films with heat treatment of 450 °C (A), 550 °C (B) and 600 °C (C). It is possible to observe that the samples have similar crystalline surfaces, with the presence of pores. The film with a sintering temperature of 450 °C appears to be more porous than the other two films.

ZOUHI *et al*. [33] mathematically analyzed the effect of TiO_2 porosity in a DSSC and concluded that an increase in porosity favors the capture of light that occurs in the working electrode and, consequently, the generation of photoexcited electrons. However, if the porosity of the film is very high, it will result in a decrease of the light absorption coefficient due to the decrease in the area available for the adsorption of the dye.
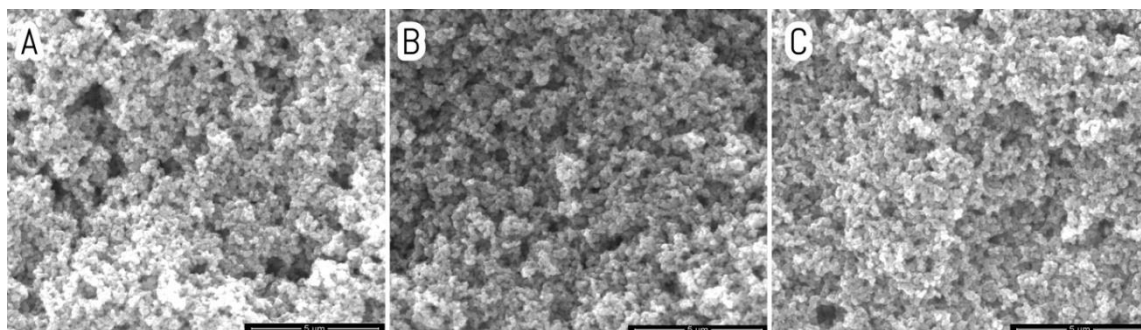
Figure 2: SEM images of TiO_2 film surfaces for sintering temperature of 450 °C (A), 550 °C (B) and 600 °C (C).

In order to avoid the formation of cracks on the surface of the films at the end of the electrophoretic deposition process, a hot air gun was used to evaporate the excess solvent. It was observed that the solvent evaporated rapidly at a temperature of 100 °C. According to SOUZA [34], cracks cause a discontinuity of the film resulting in a reduction in conductivity.

Dispersive energy spectroscopy offers information on the relative proportions of the elements found in the analyzed area. Therefore, (SEM) scanned film areas of each sample generated spectroscopies and images of the mapping areas, as shown in Figures 3, 4 and 5, corresponding to samples 450, 550 and 600 respectively-ly.
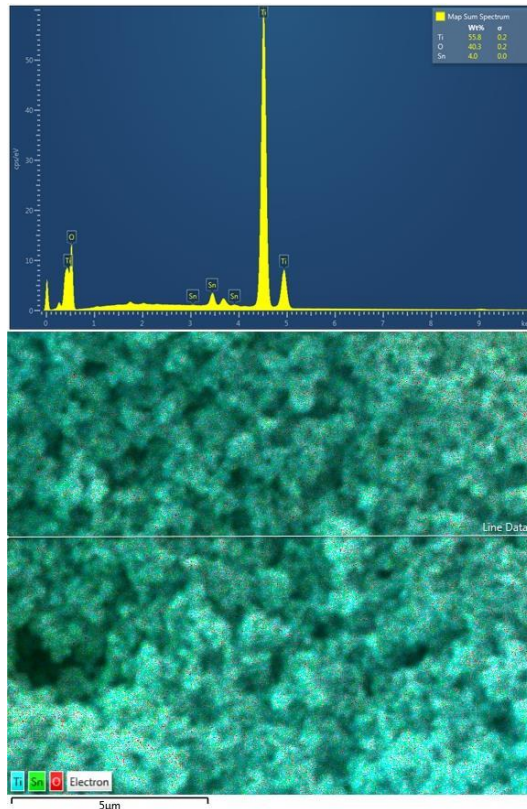
Figure 3: EDS from sample 450 with the respective mapping area.
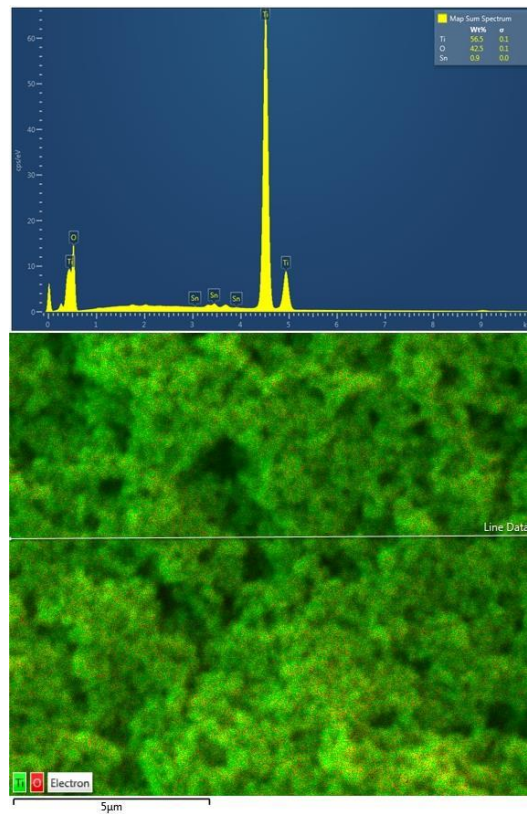
Figure 4: EDS of sample 550 with the respective mapping area.
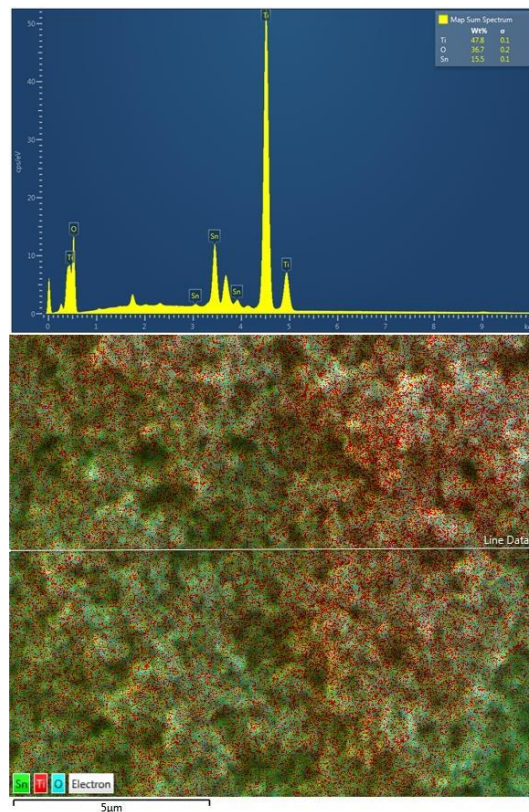
Figure 5: EDS of sample 600 with the respective mapping area.

For sample 450 the mass ratio of titanium (Ti) is 56.5%, 55.8% for sample 550 and 47.8% for sample 600. These values confirm the deposition of the TiO_2 film by electrophoresis on the substrate of FTO. The spectra confirm, in addition to titanium, the presence of oxygen (O) and tin (Sn), the latter being due to the substrate used in the deposition. These results reveal that in the three samples there was no identification of impurities present in the film.

The reduction in titanium percentages as the sintering temperature increases may indicate that the areas mapped in samples 550 and 600 have irregularities in the film. As a consequence,the thicknesses of the films in these regions are smaller, which makes it possible to identify elements of Sn and O present in the substrate.

3.2 X-ray diffraction analysis (XRD)

The XRD results for samples 450, 550 and 600 are shown in Figure 6. As the same materials were used for all samples, the peak intensities for the TiO_2 diffractogram are similar and observed in the crystallographic directions (101), (004), (200), (105), (211) and (204) which, according to HOSSAIN *et al.* [35], indicate the anatase phase. This measurement showed that the electrophoresis deposition method and the thermal treatment did not alter the crystalline structure of the material, maintaining its most active phase (anatase). This is due to the fact that the minimum temperature for the transition from anatase to rutile phase is between 700 °C - 900 °C according to FAZLI *et al.* [36].

In order to avoid fusing the FTO substrate to the sample holder, it was necessary to deposit a TiO_2 film on a platinum substrate. Thus, in the XRD results (Figure 6) peaks of tin oxide are not observed as it is normally found in films deposited on FTO. The platinum peaks identified with the (*) were obtained due to the

SOUZA, A.P.S.; CAVALCANTE, N.M.C.; FREIRE, F.N.A. *et al.*, revista Matéria, v.26, n.1, 2021

substrate used. It is worth noting that only in the X-ray diffraction measurement a different substrate was used, in the other characterization techniques the substrate used was glass with FTO.
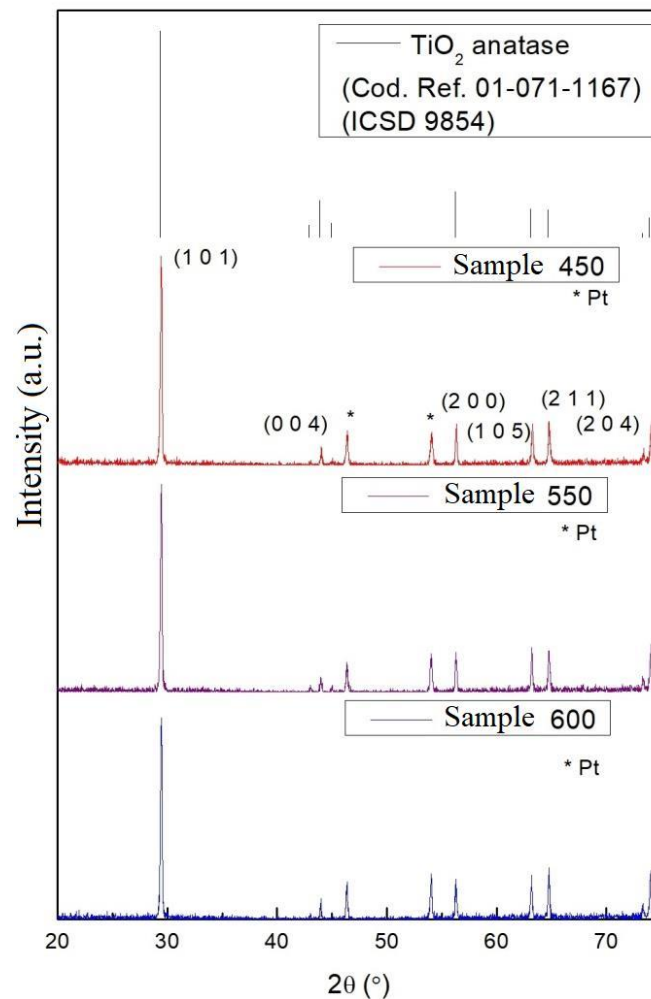
Figure 6: X-ray diffractograms of TiO$_2$ samples.

The crystallographic directions of the TiO$_2$ peaks and the platinum peaks, described in sample 450, are also similar in the other samples. This happens because there are no significant structural changes during heat treatment.

The crystallite size of the films can be calculated from the equation of Debye-Scherrer [35] given by:

$$L = \frac{K\lambda}{\beta cos\theta} \tag{2}$$

Where L is the size of the crystallite in nm, K is the Scherrer constant, λ is the wavelength of the radiation used, β is the width at half height of the diffraction peak (FWHM) in radians and θ is the Bragg angle in radians. The parameters FWHM and θ can be obtained from the XRD data of the peaks and the values of 0.9 and 0.1789 nm are used for K and λ respectively.

To obtain the values of 2θ and FWHM, the software X'Pert Higschore Plus was used, where it was possible to open the data file obtained from the DRX. In the software it is possible to obtain the list of peaks with the parameter values. The parameters and crystallite size of the peaks of each sample are summarized in Tables 2, 3 and 4.

Table 2: Parameters FWHM, θ and crystallite size of sample 450, sintered at 450 ℃

PEAKS	2Θ (°)	FWHM (°)	L (NM)
(101)	29.4558	0.1872	50.95
(004)	44.0315	0.2496	39.87
(200)	56.3365	0.1872	55.90
(105)	63.2887	0.1872	57.89
(211)	64.7503	0.1560	70.02
(204)	74.1301	0.1872	61.76

Table 3: Parameters FWHM, θ and size of crystallites in sample 550, sintered at 550 ℃

PEAKS	2Θ (°)	FWHM (°)	L (NM)
(101)	29.4484	0.1872	50.95
(004)	43.9975	0.2496	39.86
(200)	56.2450	0.1848	56.60
(105)	63,2072	0.1560	69.43
(211)	64.7503	0.1872	58.35
(204)	74.0667	0.1560	74.08

Table 4: FWHM, θ and crystallite size parameters of sample 600, sintered at 600 ℃

PEAKS	2Θ (°)	FWHM (°)	L (NM)
(101)	29,5001	0.1248	76.44
(004)	43.9917	0.1872	53.15
(200)	56.2396	0.2496	41.91
(105)	63.1920	0.1872	57.86
(211)	64.7431	0.2184	50.01
(204)	74.0396	0.1560	74.07

Tables 2, 3 and 4 show that some peaks suffered a small reduction in θ with the increase in the sintering temperature, which is not possible to observe visually in the results of the diffractograms. The crystallite sizes of sample 450 vary between 39.87 nm and 70.02 nm, of sample 550 vary between 39.86 nm and 74.08 nm and sample 600 vary between 41.91nm and 76.44nm. Thus, the sintering temperature of the films slightly influences the size of the crystallites and consequently the surface area of the TiO$_2$ films.

The size of the crystallites of the film increases slightly with the increase in the sintering temperature [37] causing a decrease in the surface area of the film [15].

3.3 Photovoltaic properties of cells

Lastly, all the photovoltaic devices showed in Figures 7, were assembled and characterized following the procedures on section 2.2.6 and 2.2.4, respectively.

The graphs of the current-voltage density plots are shown in Figures 8, 9 and 10. The photovoltaic parameters obtained for the three cells were compared and are summarized in Table 5.
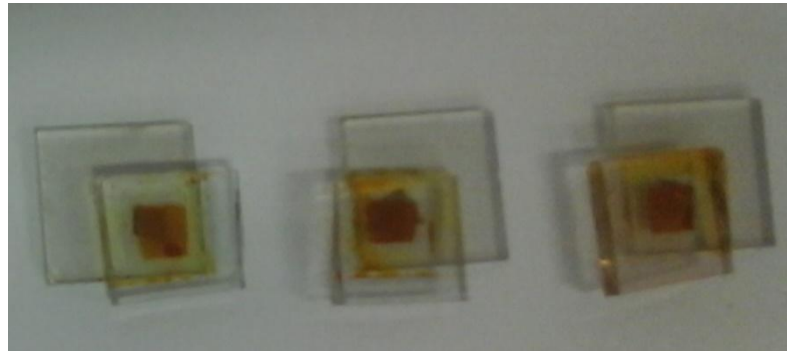
Figure 7: Assembled photovoltaic devices.
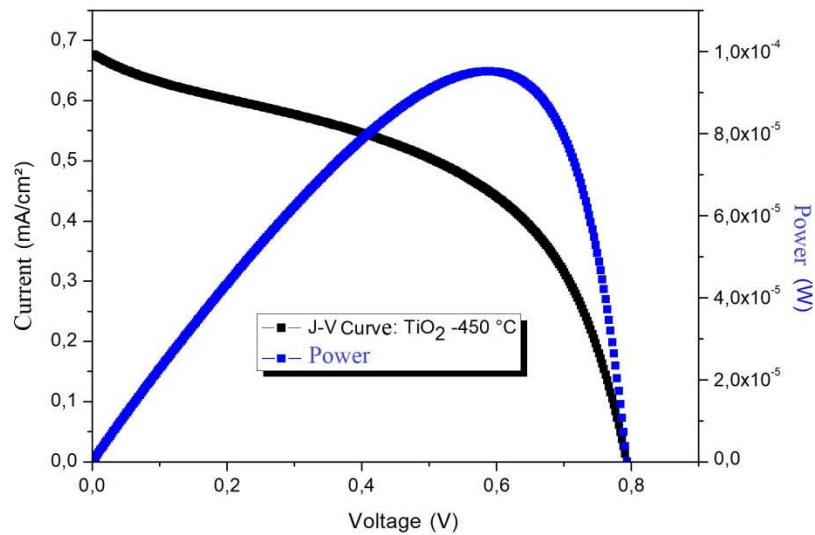
Figure 8: J-V curve of sample 450.
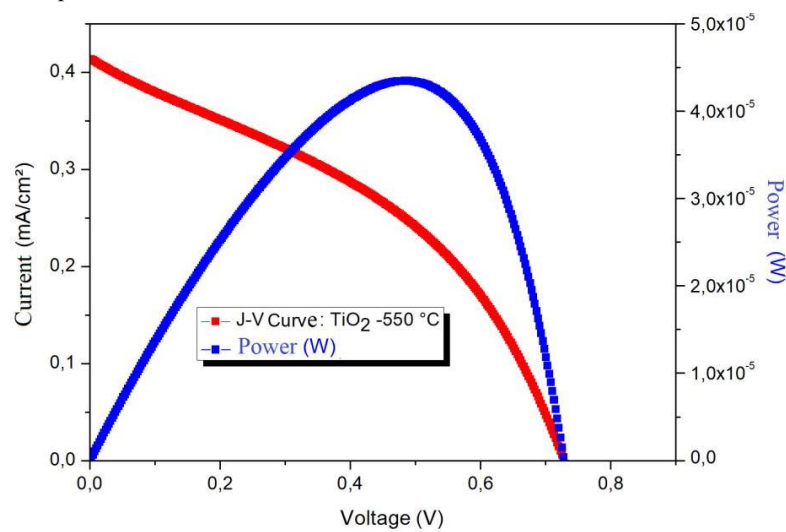
Figure 9: J-V curve of sample 550.
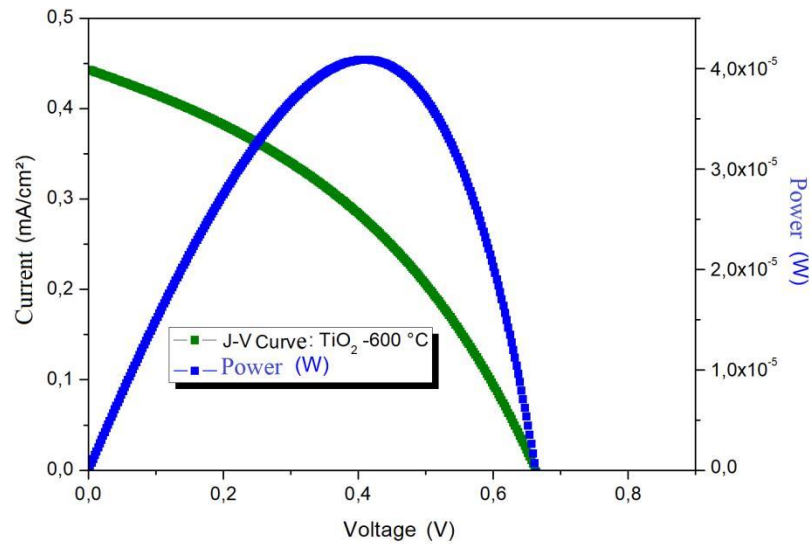
Figura 10: Curva J-V da amostra 600.

The Cells efficiencies with samples 450, 550 and 650 were calculated according to Equation 3. The parameters R_S and R_{SH} correspond to the resistances in series and in parallel, respectively, assigned to the circuit that models the photovoltaic cells.

$$\eta = \frac{V_{OC} \cdot J_{SC} \cdot FF}{P_{IN}}$$
(3)

Where, Voc is the open circuit voltage, Jsc is short-circuit current, FF it is the fill factor and P_{IN} is the radiation power incident on the cell.

Table 5: Photovoltaic parameters for TiO_2 cells.

Cells	J_{SC} (mA/cm²)	V_{OC} (V)	R_S (Ω.cm²)	R_{SH} (Ω.cm²)	FF	η (%)
450	0.68	0.79	174.41	2143.93	0.4928	0.27
550	0.41	0.73	530.43	2870.79	0.4016	0.12
650	0.44	0.66	579.57	3592.63	0.3868	0.11

The short circuit current density (J_{SC}) decreased with the increase in the sintering temperature of the film and the highest value was obtained by the cell that had the highest efficiency. The amount of electrons generated by the dye determines the current generated. Therefore, the greater the amount of dye adsorbed on the film, the greater the generation of electrons and consequently the current density will, also, be greater. [36] Cell with the sample 450 was the one with the highest current density value, indicating that the TiO_2 film sintered at 450 °C possibly obtained the highest amount of adsorbed dye. This result is in accordance with the values of the calculation of the sizes of crystallites performed previously, which found that sample 450 had a greater surface area and consequently a greater adsorption of dye.

According to NONO [38], the open circuit potential (V_{OC}) depends on the ratio between the amount of electrons injected into the semiconductor and the amount of electrons that undergo recombination on the electrode or electrolyte surface. Table 5 shows that for the highest sintering temperature, the lowest V_{OC} value was obtained, which indicates that in this cell a greater load recombination may have occurred, resulting in a lower efficiency.

The fill factor (FF) decreases as the sintering temperature increases. One of the main factors that influence the value of the FF is the series resistance (R_S) inside the cell that will directly affect the electron transfer process. SOUZA *et al.* [15], SEQUEIRA [39] and NUNES [40], also observed in their experiments that solar cells that had higher Rs values, had lower FF values.

The energy conversion efficiencies obtained for the cells were 0.2664% for the cell containing sample 450, 0.1209% for the cell containing sample 550 and 0.1137% for the cell containing sample 600.

According to CHANG *et al.* [41], the efficiency of the cell is also affected by the uniformity of the film thickness, and the non-uniformity results in reduced efficiencies due to recombination of charges.

Other studies have also reported dye-sensitized solar cells with efficiencies of less than 1% such as that made by CHIANG, LEE and HSU [42] and AZIZI *et al.* [43]. CHIANG, LEE and HSU [42] assembled cells with titanium dioxide deposited by electrophoresis and doctor blade on ITO substrates and obtained efficiencies of 0.0473% and 0.1327%, respectively. AZIZI *et al.* [43] deposited a TiO_2 film by electrophoresis on an FTO substrate, which underwent heat treatment at 450 ° C. In assembling the cells, different natural dyes were used and the efficiencies obtained varied between 0.007% and 0.09%.

The low efficiency found in this work was caused by high values of resistance in series (Rs) with reduction in the conductivity of the cell. This problem can be reduced with the chemical treatment of the films with $TiCl_4$. The electrical conductivity has been improved at the interfaces between particles in the TiO_2 coating and between conducting glass and the TiO_2 film through $TiCl_4$ treatment. [44-50]

4. CONCLUSIONS

The electrophoresis dispersion and deposition process proved to be a promising technique in the construction of porous films for application in DSSCs. The XRD analyzes of all samples indicated similarity in the crystallographic directions that correspond to the anatase phase of TiO_2, confirming that the electrophoresis deposition method and the heat treatment did not alter the crystalline structure of the material. It was verified through the analysis of XRD data the influence of the sintering temperature on the size of the crystallites, which suggests that the size of the crystallites increases slightly with the increase of the sintering temperature. The result of this reduction in the surface area of the film may cause a lesser injection of electrons for the semiconductor oxide, due to the lower amount of dye adsorbed on the surface of this oxide. The film sintered at 450 °C showed smaller crystallites, which contributed to increasing the efficiency of this cell.

SEM analysis revealed that all films had crystalline surfaces with the presence of pores. The film sintered at 450 °C showed greater porosity compared to the other two. The EDS spectra showed that all films contained only titanium and oxygen, confirming that the electrophoresis deposition technique was efficient. There was a reduction in the mass proportions of titanium and an increase in the proportions of tin as the sintering temperature increased, indicating a possible variation in the thickness of the film.

From the parameters obtained from the current-voltage plots it was possible to calculate the efficiency of the cells. The cell with TiO_2 film sintered at 450 °C presented the highest efficiency value, 0.2664%. This greater efficiency is due to the fact that the film had larger surface area, which results in greater dye adsorption and greater electron generation. In order to optimize the photovoltaic capacity of solar cells sensitized by dyes with TiO_2 films deposited by electrophoresis, it is suggested to carry out analyzes

involving post-treatment with TiCl₄ of the electrophoretically deposited films, in addition to the variation of deposition parameters and sintering temperature.

5. ACKNOWLEDGMENTS

6. BIBLIOGRAPHY

[1] JOSE, R., THAVASI, V., "Ramakrishna, Metal oxides for dye-sensitized solar cells", *Jornal of the. American Ceramic Society*. v.92, pp. 289-301, 2009.

[2] HU, Y., TSAI, H.L., HUANG, C.L., "Effect of brookite phase on the anatase-rutile transition in titania nanoparticles", *Jornal of the European Ceramican. Society*. v.23, pp. 691–696, 2003.

[3] PAN, H., GU, B., ZHANG, Z. "Phase-dependent photocatalytic ability of TiO₂: a first principles study", *Jornal of Chemical Theory and Computation*, v.5, pp. 3074-3078, 2009.

[4] VIEIRA, F.T.G., MELO, D.S., LIMA, S.J.G., *et al.,* "The influence of temperature on the color of TiO₂:Cr pigments", *Materials Research Bulletin*, v.44, pp. 1086-1092, 2009.

[5] ZHUANG, J., DAI, W., TIAN, Q. *et al.,* "Photocatalytic degradation of RhB over TiO₂ bilayer films: effect of defects and their Location", ***Langmuir:** American Chemical Societ,* v.26, pp. 9686–9694, 2010.

[6] SEO, M.H., YUASA, M., KIDA, T. *et al.,* "Detection of organic gases using TiO₂ nanotube-based gas sensors", *Procedia Chemistry: Jornal*, v.1, pp. 192-195, 2009.

[7] LABILLI, J., FENG, J., BOTTA, C., *et al.,* "Aging of TiO₂ nanocomposites used in sunscreen Dispersion and fate of the degradation products in aqueous environment", *Environmental. Pollution: Jornal*, v.158, pp. 3482-3489, 2010.

[8] GRINIS, L., DOR, S., OFIR, A., *et al.,* "Electrophoretic deposition and compression of titania nanoparticle films for dye-sensitized solar cells", *Jornal Photochemitry. Photobiology. A: Chem*, v.198, pp. 52-59, 2008.

[9] HILLHOUSE, H.W., BEARD, M.C. "Solar cells from colloidal nanocrystals: fundamentals, materials, devices, and economics", *Current Opinion in Colloid Interface Sci:Jornal*, v.14, pp. 245-259, 2009.

[10] CHEN, Z.H., TANG, Y.B., LIU, C.P. *et al.,* "Vertically aligned ZnO nanorod arrays sentisized with gold nanoparticles for schottky barrier photovoltaic cells", *The Jornal of Physical Chemistry C*, v.113, pp. 13433-13437, 2009.

[11] MARTINSON, A.B.F., GOES, M.S., FABREGAT-SANTIAGO, F., *et al.,* "Electron Transport in Dye-Sensitized Solar Cells Based on ZnO Nanotubes: Evidence for Highly Efficient Charge Collection and Exceptionally Rapid Dynamics", *The Jornal of Physical Chemistry A*, pp. 4015-4021, v.113, 2009.

[12] KAY, A., GRATZEL, M. "Dye-Sensitized Core-Shell Nanocrystals: Improved Efficiency of Mesoporous Tin Oxide Electrodes Coated with a Thin Layer of an Insulating Oxide". *Chemistry of Materials*, pp. v. 14, 2930-2935, 2002.

[13] MENDE, S., BACH, U., BAKER, H., *et al.,* Organic dye for highly efficient solid-state dye-sensitized solar cells. Advanced Materials**.** v.17, p.813, 2005.

[14] CHANG, Y.J., CHOW, T.J. "Highly efficient triarylene conjugated dyes for sensitized solar cells". *Journal of Materials Chemistry***.** v.21, p.9523, 2011.

[15] SOUZA, A.P.S., FERREIRA, O.P., NUNES, V.F., *et al.,* "Performance Evaluation of Titanate Nanotubes and Nanoribbons Deposited by Electrophoresis in Photoelectrodes of Dye-Sensitized Solar Cells", *Materials Research*, [s.l.], v. 21, n. 4, 28 maio 2018.

[16] O'REGAN, B., MICHAEL, G.. "A low-cost, high-efficiency solar cell based on dyesensitized colloidal TiO₂ films". *Nature*, v.353, p.737-740, 1991.

[17] SONG, M.Y., KIM, D.K., JO, S.M. *et al.,* "Enhancement of the photocurrent generation in dye-sensitized solar cell based on electrospun TiO_2 electrode by surfasse Treatment", *Synthstic Metals:Jornal*, v.155, pp. 635-638, 2005.

[18] HOSSAIN, M.F., BISWAS, S., TAKAHASHI, T. *et al.,* "Investigation of sputter-deposited TiO_2 thin film for the fabrication of dye-sensitized solar cells", *Thin Solid Films*, v. 516, pp. 7149-7154, 2008.

[19] WANG, S., WU, X., QIN, W. *et al.* "TiO_2 films prepared by micro-plasma oxidation method for dye-sensitized solar cell", *Electrochimical Acta,* v.53, pp.1883-1889, 2007.

[20] ZHITOMIRSKY, I. "Cathodic electrophoretic deposition of ceramic and organoceramic materials – fundamental aspects", *Advances in Colloid and Interface Science*, v.97, pp.279-317, 2002.

[21] HEAVENS, N. "Electrophoretic deposition as a processing route for ceramics". In: Binner GP, editor. *Advanced ceramic processing and technology*, v. 1, p. 255-83, 1990.

[22] BESRA, L., LIU, M.. "A review on fundamentals and applications of electrophoretic deposition (EPD)". *Progress in Materials Science.* v.52, pp.1-61, 2007.

[23] MOSKALEWICZ, T., CZYRSKA-FILEMONOWICZ, A. Microstructure of nanocrystalline TiO_2 films produced by electrophoretic deposition on Ti–6Al–7Nb alloy. *Surface and Coatings Technology.* v. 21, pp. 7467-7471, May 2007.

[24] HAMADANIAN, M., JABBARI, V., GRAVAND, A., *et al.,* Band gap engineering of TiO_2 nanostructure-based dye solar cells (DSCs) fabricated via electrophoresis. *Surface and Coatings Technology.* v. 206, Issue 22, pp. 4531-4538, 25 June 2012.

[25] KIMURA, T., TAKENAKA, T., FUJITSU, S., *et al.,* Preparation of TiO_2 Thin Film for Dye Sensitized Solar Cell Deposited by Electrophoresis Method. v. 248, pp. 133-136, Aug. 2003.

[26] VITTAL, R., HO KC. "Zinc oxide based dye-sensitized solar cells": *A review. Renewable and Sustainable Energy Reviews.*, v.70, pp.920-935, 2017.

[27] SOLEMS L'ÉNERGIE LUMIÉRE®, Transparent conductive oxides (TCO) thin films on glass, FT-TCO en/ 2015-1, p.1-2. www.solems.com.

[28] LIU, J., LI, Y., ARUMUGAM, S., *et al.,* Investigation of Low Temperature Processed Titanium Dioxide (TiO_2) Films for Printed Dye Sensitized Solar Cells (DSSCs) for Large Area Flexible Applications. *Materials Today*: *Proceedings.* v.5, pp.13846-13854, (2018).

[29] THE-VINH NGUYEN HYUN-CHEOL LEE O-BONG YANG. The effect of pre-thermal treatment of TiO_2 nano-particles on the performances of dye-sensitized solar cells. *Materiais de energia solar e células solares.* v. 90, pp. 967-981, may, 2006.

[30] SOUZA, A.P.S, ALMEIDA, A.F.L.,CONEGERO, L.S., *et al.,* Photoelectrodes with titanate nanotubes sensitized by mesoporphyrin derivative from cashew nut shell. *Matéria (Rio J.)*, ISSN 1517-7076, v.24, n.1. 2019.

[31] ITO, S., TAKEUCHI, T., KATAYAMA, T., *et al.,* Conductive and Transparent Multilayer Films for Low-Temperature-Sintered Mesoporous TiO_2 Electrodes of Dye-Sensitized Solar Cells, *Chemistry of Materials.* v.15, n. 14, pp.2824-2828, 2003.

[32] SOLARONIX®, Dye Solar Cells for Real-Innovative Solutions for Solar Professionals. http://www.solaronix.com/documents/solaronix_materials.pdf, p.8-37, Switzerland, 2012.

[33] ZOUHRI, K., ALSADI, J., FERREIRA, L., *et al.,* "Numerical method of the TiO_2 porosity effect on dye sensitized solar cell exergy efficiency". *Solar Energy*, v. 155, p.920-933, out. 2017.

[34] SOUZA, A.P.S. "*Produção e Caracterização de Células Solares Fotossensibilizadas por Corante Baseadas em Filmes Finos de Titanatos e Óxidos Metálicos Nanoestruturados*".Tese de Doutorado-Departamento de Pós-Graduação em engenharia e Ciência de Materiais-Universidade Federal do Ceará. Fortaleza, 2019.

[35] HOSSAIN, M.K., MOTRUZA, A.A., SEN, S.K., *et al.,* "A comparative study on the influence of pure anatase and Degussa-P25 TiO_2 nanomaterials on the structural and optical properties of dye sensitized solar cell (DSSC) photoanode". *Optik*, v. 171, p.507-516, out. 2018.

[36] FAZLI, F.I.M., AHMAD, M.K., LOGO, C.F., *et al.,*"Dye-sensitized solar Cell using pure anatase TiO_2 annealed at different temperatures". *Optik*, v. 140, p.1063-1068, jul. 2017.

[37] ZHOU, M., YU, J., LIU, S., *et al.,* "Effects of calcination temperatures on photocatalytic activity of SnO_2/TiO_2 composite films prepared by an EPD method". *Journal of Hazardous Materials*, v. 154, n. 1-3, p.1141-1148, jun. 2008.

[38] NONO, R.S. *Preparação de filmes de TiO2 para aplicação em células solares de corante*. 2005. 75 f. Dissertação (Mestrado) - Curso de Química, Departamento de Química Inorgânica, Universidade Estadual de Campinas, Campinas, 2005.

[39] SEQUEIRA, S.I.H. *Células solares sensibilizadas por novos corantes derivados de cumarinas*. 2012. 89 f. Dissertação (Mestrado) - Curso de Engenharia da Energia e do Ambiente, Universidade de Lisboa, Lisboa, 2012.

[40] NUNES, V.F. *Síntese e caracterização de células solares de ZnO sensibilizadas por corante*. 2018. 56 f. Dissertação (Mestrado) - Curso de Engenharia Mecânica, Universidade Federal do Ceará, Fortaleza, 2018.

[41] CHANG, H., SU, H.T, CHEN, W.A, *et al.,* Fabrication of multilayer TiO_2 thin films for dye-sensitized solar cells with high conversion efficiency by electrophoresis deposition". Solar *Energy*, v. 84, n. 1, pp.130-136, jan. 2010.

[42] CHIANG, W.T., LEE, P.T., HSU, R.Q. "Study on Preparation of Flexible Semiconductor Electrode for Dye-sensitized Solar Cells by EPD*". Manufacturing Science And Technology*, v. 3, n. 4, pp.170-176, dez. 2015.

[43] AZIZI, T., TOUIHRI, A.E., KAROUI, M.B., *et al.,* "Comparative study between dye-synthesized solar cells prepared by electrophoretic and doctor blade techniques". *Optik*, v. 127, n. 10, pp.4400-4404, maio 2016.

[44] SEDGHI, A., MIANKUSHKI, H.N.. "Influence of $TiCl_4$ Treatment on Structure and Performance of Dye-Sensitized Solar Cells Jpn". *Jornal of Applicated Physical*. v.52, p. 075002, 2013.

[45] NATH, N.C.D., SUBRAMANIAN, A., HU, R.Y., *et al.,* "Effects of $TiCl_4$ Post-Treatment on the Efficiency of Dye-Sensitized Solar Cells". *Journal of Nanoscience and Nanotechnology*, v. 15, pp. 8870-8875, 2015. doi:10.1166/jnn.2015.11528.

[46] KABIR, F., BHUIYAN, M.H., Md ROBIUL HOSSAIN, *et al.,* "Effect of combination of natural dyes and post-$TiCl_4$ treatment in improving the photovoltaic performance of dye-sensitized solar cells". *Comptes Rendus Chimie: Jornal*. doi.org/10.1016/j.crci.2019.08.002, v.22, pp. 659-666, Issues 9-10, September-October 2019.

[47] ADHIKARI, S.G., SHAMSALDEEN, A., ANDERSSON, G.G.. "The effect of $TiCl_4$ treatment on the performance of dye-sensitized solar cells". *Jornal of Chemistry and Physcal*. doi.org/10.1063/1.5125996. v.151, pp.164704, 2019.

[48] SOMMELING, P.M., O'REGAN, B.C., HASWELL, R.R., *et al.,* "Influence of a $TiCl_4$ Post-Treatment on Nanocrystalline TiO_2 Films in Dye-Sensitized Solar Cells". Jornal of Physical and Chemistry B, doi.org/10.1021/jp061346k. v.110, pp.19191-19197, 2006.

[49] MURAKAMI, T.N., MIYADERA, T., FUNAKI, T. *et al.,* "Adjustment of Conduction Band Edge of Compact TiO_2 Layer in Perovskite Solar Cells Through $TiCl_4$ Treatment". *ACS Applied Materials&Interfaces*, doi: 10.1021/acsami.7b07496. v.9, pp.36708-36714, 2017.

[50] YAHAV, S., RÜHLE, S., GREENWALD, S., *et al.,* "Strong Efficiency Enhancement of Dye-Sensitized Solar Cells Using a La-Modified $TiCl_4$ Treatment of Mesoporous TiO_2 Electrodes". *The Journal of Physical Chemistry C*, doi: 10.1021/jp2042679. *v.*115*,* pp.21481-21486, 2011.

ORCID

Antonio Paulo Santos Souza   https://orcid.org/0000-0001-8518-0503
Natália Macêdo Cavalcante   https://orcid.org/0000-0002-2064-5581
Francisco Nivaldo Aguiar Freire   https://orcid.org/0000-0001-5449-2635
Ana Fabíola Leite Almeida   https://orcid.org/0000-0002-8867-5453